Liquid-liquid interfacial properties of a symmetrical Lennard-Jones binary mixture

F. J. Martínez-Ruiz, A. I. Moreno-Ventas Bravo, and F. J. Blas

Citation: The Journal of Chemical Physics **143**, 104706 (2015); doi: 10.1063/1.4930276
View online: http://dx.doi.org/10.1063/1.4930276
View Table of Contents: http://scitation.aip.org/content/aip/journal/jcp/143/10?ver=pdfcov
Published by the AIP Publishing

Liquid-liquid interfacial properties of a symmetrical Lennard-Jones binary mixture

F. J. Martínez-Ruiz,[1] A. I. Moreno-Ventas Bravo,[2] and F. J. Blas[1,a)]
[1]*Laboratorio de Simulación Molecular y Química Computacional, CIQSO-Centro de Investigación en Química Sostenible and Departamento de Física Aplicada, Universidad de Huelva, 21007 Huelva, Spain*
[2]*Laboratorio de Simulación Molecular y Química Computacional, CIQSO-Centro de Investigación en Química Sostenible and Departamento de Geología, Universidad de Huelva, 21007 Huelva, Spain*

(Received 13 June 2015; accepted 26 August 2015; published online 14 September 2015)

We determine the interfacial properties of a symmetrical binary mixture of equal-sized spherical Lennard-Jones molecules, $\sigma_{11} = \sigma_{22}$, with the same dispersive energy between like species, $\epsilon_{11} = \epsilon_{22}$, but different dispersive energies between unlike species low enough to induce phase separation. We use the extensions of the improved version of the inhomogeneous long-range corrections of Janeček [J. Phys. Chem. B **110**, 6264 (2006)], presented recently by MacDowell and Blas [J. Chem. Phys. **131**, 074705 (2009)] and Martínez-Ruiz *et al.* [J. Chem. Phys. **141**, 184701 (2014)], to deal with the interaction energy and microscopic components of the pressure tensor. We perform Monte Carlo simulations in the canonical ensemble to obtain the interfacial properties of the symmetrical mixture with different cut-off distances r_c and in combination with the inhomogeneous long-range corrections. The pressure tensor is obtained using the mechanical (virial) and thermodynamic route. The liquid-liquid interfacial tension is also evaluated using three different procedures, the Irving-Kirkwood method, the difference between the macroscopic components of the pressure tensor, and the test-area methodology. This allows to check the validity of the recent extensions presented to deal with the contributions due to long-range corrections for intermolecular energy and pressure tensor in the case of binary mixtures that exhibit liquid-liquid immiscibility. In addition to the pressure tensor and the surface tension, we also obtain density profiles and coexistence densities and compositions as functions of pressure, at a given temperature. According to our results, the main effect of increasing the cut-off distance r_c is to sharpen the liquid-liquid interface and to increase the width of the biphasic coexistence region. Particularly interesting is the presence of a relative minimum in the total density profiles of the symmetrical mixture. This minimum is related with a desorption of the molecules at the interface, a direct consequence of a combination of the weak dispersive interactions between unlike species of the symmetrical binary mixture, and the presence of an interfacial region separating the two immiscible liquid phases in coexistence. [http://dx.doi.org/10.1063/1.4930276]

I. INTRODUCTION

Interfacial tension is probably the most challenging property to be determined and predicted using computer simulation techniques.[1] Despite the number of studies carried out since computer simulation is used routinely for determining the properties of a molecular model, the calculation of interfacial tension is still a subtle problem. The ambiguity in the definition of the microscopic components of the pressure tensor,[2,3] the finite size effects due to capillary waves,[4,5] or the difficulty for the calculation of the dispersive long-range corrections (LRC) associated to the intermolecular interactions[6,7] make the calculation of interfacial tension a difficult and non-trivial problem.

The standard methodology used to determine the fluid-fluid interfacial tension in a molecular simulation involves the determination of the microscopic components of the pressure tensor, i.e., the normal and tangential pressure, $P_N(z)$ and $P_T(z)$, respectively, through the well-known mechanical or virial route. Once both components are determined, the interfacial tension of a planar fluid-fluid interface can be readily obtained from the integration of the difference between the normal and tangential microscopic components of the pressure tensor profiles along the interface,

$$\gamma = \int_0^{L_z} (P_N(z) - P_T(z))\, dz. \tag{1}$$

Note that the z-axis is chosen perpendicular to the interface and the integral is performed along the total length L_z of the simulation box. Care must be taken in cases in which there exist two fluid-fluid interfaces, which is the standard procedure for studying direct fluid-fluid coexistence in Monte Carlo (MC) and Molecular Dynamics (MD) simulation. In this case, the true value associated to a single interface is half of the value obtained from Eq. (1). This method generally involves an ensemble average of the virial of Clausius according to the recipes of Irving and Kirkwood (IK).[8]

a)Electronic mail: felipe@uhu.es

Although the mechanical route is an appropriate technique for determining the interfacial tension, a number of alternative methods have been proposed during the last years to calculate not only the interfacial tension but also for the components of the pressure tensor, without the need to evaluate the virial. These new effective and elegant methods are based on the thermodynamic definition of surface tension and pressure tensor. The first one can be understood as the change in free energy when the interfacial area is changed, at constant volume and temperature. The second one can be expressed as the change in free energy when the volume of the system is changed along any direction, keeping constant the other two dimensions. Examples of these methods are the Test-Area (TA) technique of Gloor *et al.*,[3] the Volume Perturbation (VP) method of de Miguel and Jackson,[9–11] the Wandering Interface Method (WIM), introduced by MacDowell and Bryk,[12] and the use of the Expanded Ensemble (EE), based on the original work of Lyuvartsev *et al.*,[13] for calculating the surface tension proposed independently by Errington and Kofke[14] and de Miguel.[15] These methods are becoming very popular and are being used routinely to determine the vapour-liquid (VL) interfacial properties of different potential model fluids.[7,16–35]

As mentioned previously, one of the major difficulties encountered in the simulation of inhomogeneous systems by molecular simulation is the truncation of the intermolecular potential. Although for homogeneous systems this issue is easily solved by including the well-known homogeneous LRC,[36,37] the situation is much more complicated in the case of fluid-fluid interfaces, and in general, in inhomogeneous systems. Fortunately, this problem seems to be solved satisfactorily recently in cases in which the system exhibits planar symmetry. Different authors have contributed to the establishment of appropriate and standard inhomogeneous LRC, including Blokhius,[38] Mecke,[39,40] Daoulas,[41] Guo and Lu,[42] and finally, Janeček,[6,43] and the recent improved methods proposed by MacDowell and Blas,[7] de Gregorio *et al.*,[33] and Martínez-Ruiz *et al.*[34,35]

Despite the great number of studies carried out during the last 10 years for determining the interfacial tension and pressure tensor from Monte Carlo and molecular dynamics methodologies, most of them have focused on using the mechanical or virial route for determining these properties. Little work, however, has been developed to determine the interfacial properties, and particularly the surface tension and pressure tensor, from perturbative and thermodynamic methods for binary mixtures involving liquid-liquid (LL) separation. An important exception is the work of Neyt *et al.*,[31] in which oil-water liquid-liquid interfaces are investigated using atomistic and coarse grained force fields.

The goal of this work is twofold. The first objective is to determine the liquid-liquid interfacial properties of a symmetrical binary mixture of equal-sized LJ spheres, $\sigma_{11} = \sigma_{22}$, with dispersive energies of equal strengths between like species, $\epsilon_{11} = \epsilon_{22}$, but with the dispersive energy between unlike species low enough to induce phase separation, $\epsilon_{12} = 0.5\epsilon_{11}$. The phase behavior of the system is dominated by large regions of liquid-liquid coexistence brought about by the small value of unlike dispersive interaction in comparison with the strengths between like species ($\epsilon_{11} = \epsilon_{22}$). In particular, we focus on the effect of the cut-off distance of the intermolecular potential energy, r_c, on different interfacial properties, including density profiles, normal and tangential microscopic components of the pressure tensor profiles, and interfacial tension. In addition to that, we also analyze the effect of the cut-off distance on other thermodynamics properties, such as coexistence density and pressure-composition projection of the phase diagram. The second objective is to check the accuracy of the improved versions of the inhomogeneous LRC of Janeček[6] recently proposed by MacDowell and Blas[7] for the intermolecular energy and Martínez-Ruiz *et al.*[34,35] for the microscopic components of the pressure tensor. In order to check the effectiveness of these methods in the case of a mixture that exhibits liquid-liquid phase separation, we also determine the interfacial tension and the components of the pressure tensor using two different perturbative methods, the TA technique and the VP methodology. This allows to obtain independent results and compare our predictions with simulation data taken from the literature. To our knowledge, this is the first time the interfacial tension and components of the pressure tensor of a symmetrical mixture of LJ spheres are calculated using perturbative methods in both cases and taking into account the LRC associated to the intermolecular potential and components of the pressure tensor.

The rest of the paper is organized as follows. In Section II, we present the model and simulation details of this work. Results obtained are discussed in Section III. Finally, in Section IV, we present the main conclusions.

II. MODEL AND SIMULATION DETAILS

As we have mentioned in the Introduction, the simplest model mixture incorporating both attractive and repulsive dispersive interactions which displays liquid-liquid immiscibility is a binary mixture of equal-sized LJ spheres, $\sigma_{11} = \sigma_{22} \equiv \sigma$, with dispersive energies of equal strengths between like species, $\epsilon_{11} = \epsilon_{22} \equiv \epsilon$, but with the dispersive energy between unlike species low enough to induce phase separation. In this work, we consider this simple symmetrical binary mixture.

The interaction potential between any pair of molecules of species i and j is given by

$$u_{ij}^{LJ}(r) = 4\epsilon_{ij}\left[\left(\frac{\sigma_{ij}}{r}\right)^{12} - \left(\frac{\sigma_{ij}}{r}\right)^{6}\right], \tag{2}$$

where r is the distance between two molecules, and σ_{ij} and ϵ_{ij} are the intermolecular parameters (size and dispersive energy) associated to the interaction between molecules of type i and j. Since all the molecules considered are of equal-sized LJ spheres, we use the well-known Lorentz combining rule for unlike molecular size,

$$\sigma_{ij} = \frac{\sigma_{ii} + \sigma_{jj}}{2}. \tag{3}$$

Note that $\sigma_{11} = \sigma_{22} = \sigma_{12} \equiv \sigma$. In addition to that, we also fix the unlike dispersive energy $\epsilon_{12} = 0.5\epsilon$.

During the simulation, we use a potential spherically truncated (but not shifted) at a cut-off distance r_c, defined by

$$u_{ij}(r) = u_{ij}^{LJ}(r)\,[1 - \Theta(r - r_c)] = \begin{cases} u_{ij}^{LJ}(r) & r \le r_c \\ 0 & r > r_c \end{cases}, \qquad (4)$$

where $\Theta(x)$ is the Heaviside step function. Note that since we restrict our study to binary mixtures with the same size, σ, we also use the same cut-off distance r_c for all the interactions.

We examine the symmetrical mixture interacting with this spherically truncated potential model with two different cut-off distances, $r_c = 3$ and 4σ. In addition to that, we also consider a cut-off distance $r_c = 3\sigma$ with LRC for the interaction energy and pressure. Standard homogeneous LRC to both magnitudes[37] are used in *NPT* simulations of bulk phases. In addition to that, inhomogeneous LRC using the MacDowell and Blas[7,44] methodology for the intermolecular potential energy and the recipe presented in our recent paper,[34] based on the Janeček's method[6,43] for the evaluation of the LRC for the components of the pressure tensor, are used. Results obtained using these LRC are equivalent to use the full potential or a potential with infinite truncation distance.

The number of molecules, N, used in the simulations performed in this work for studying the liquid-liquid interface of the symmetrical mixture varied from $N = 2688$, for the lowest pressure considered ($P^* = P\sigma^3/\epsilon \approx 1.5$), to $N = 3216$, for the highest pressure analyzed ($P^* = P\sigma^3/\epsilon \approx 3.5$). Note that it is not possible to have systems with the same total number of molecules and with the same interfacial area since we are dealing with binary mixtures in which composition must be taken into account. Whereas the initial setup for simulations of vapour-liquid interfaces for pure systems is relatively easy, the initial configuration of a vapour-liquid or liquid-liquid interface involving a binary mixture is a delicate issue. To obtain the initial interfacial simulations boxes at different pressures, we follow the approach used in our previous paper[35] and use first the well-known soft-statistical associating fluid theory (SAFT) approach, based on Wertheim's thermodynamic perturbation theory,[45–48] and developed by Blas and Vega,[55,56] to calculate the complete phase diagram of this symmetrical mixture. The soft-SAFT approach and the different versions of this successful theoretical framework for predicting the phase behavior of complex mixtures, are well-known equations of state based on a molecular theory and have been explained and applied extensively during the last 25 yr. If the reader is interested on the details and foundations of the approach, we recommend the excellent reviews existing in the literature.[49–53]

The soft-SAFT approach, in the case of mixtures of spherical LJ molecules, reduces to the well-know Johnson *et al.* equation of state.[54] This equation is an extended Benedict-Webb-Rubin equation of state that was fitted to simulation data for the Lennard-Jones fluid. The use of this theory allows to have an initial precise picture of the coexistence envelope of the system at thermodynamic conditions at which the simulations are performed. In particular, initial densities and compositions of each component of the mixture in both liquid phases are obtained using the soft-SAFT approach for the mixtures considered in this work. We account for a detailed picture of the phase behavior of the symmetrical mixture in Section III.

Simulations are performed in two steps. In the first step, both homogeneous liquid phases, at a given temperature, $T^* = k_BT/\epsilon = 1.5$, and several pressures, are equilibrated in a rectangular simulation box of dimensions $L_x = L_y = 10\sigma$, and varying L_z. Box length measured along the z-axis is chosen in such a way that the corresponding densities match the predictions obtained from the soft-SAFT approach at temperature and pressure selected. In addition to that, the particular number of molecules of each species, in both liquid phases, is also selected according to the SAFT predictions. Both simulation boxes are equilibrated at the same temperature and pressure using an $NP_z\mathcal{A}T$ ensemble in which L_x and L_y or the interfacial area, $\mathcal{A} = L_xL_y$, is kept constant and only L_z is varied along the simulation. $NP_z\mathcal{A}T$ simulations of homogeneous phases are organized by cycles. A cycle is defined as N trial moves (displacement of the particle position) and an attempt to change the box length along the z-axis (L_z). The magnitude of the appropriate displacement is adjusted so as to get an acceptance rate of 30% approximately. We use periodic boundary conditions and minimum image convention in all three directions of the simulation box. In addition to that, homogeneous LRC to the intermolecular energy and pressure are also used.[37]

In a second step, the interfacial simulation box is prepared leaving one of the previous homogeneous liquid phases (i.e., liquid 2 or L_2) at the center of the new box with the same homogeneous liquid phase boxes (i.e., liquid 1 or L_1) of half size along the z-axis previously prepared at each side. Since L_x and L_y are the same for all homogeneous phases, it is always possible to build up the interfacial simulation box as explained here. The final overall dimensions of the L_1–L_2–L_1 simulation box are therefore $L_x = L_y = 10\sigma$ and $L_z \approx 40\sigma$ for all the pressures considered. It is worthy to note that liquid-liquid interfaces are usually thinner than vapour-liquid interfaces, and consequently, shorter interfacial simulation box along the z-axis is necessary to simulate such an interface.

The simulations for studying the liquid-liquid interface are also organized in cycles. Note that the simulations of the liquid-liquid interface are performed in the *NVT* or canonical ensemble. We use periodic boundary conditions and minimum image convention in all three directions of the simulation box. To be consistent with simulations performed using the $NP_z\mathcal{A}T$ ensemble for preparing the definitive simulation box, we use inhomogeneous LRC to the intermolecular energy of MacDowell and Blas[7,44] methodology for the intermolecular potential energy and the recipe presented in our previous paper[34] for the evaluation of the LRC for the components of the pressure tensor, both of them based on the Janeček's method.[6]

We have obtained the normal and tangential microscopic components of the pressure tensor from the mechanical expression or virial route following the same procedure as in our previous works[34,35] and used the well-known IK recipe[8,57] for determining the microscopic components of the pressure tensor, $P_N(z) \equiv P_{zz}(z)$ and $P_T(z) \equiv P_{xx}(z) \equiv P_{yy}(z) \equiv \frac{1}{2}(P_{xx}(z) + P_{yy}(z))$. The components of the pressure tensor are calculated each cycle.

Following de Miguel and Jackson,[9] we have also determined the macroscopic components of the pressure tensor

using its thermodynamic definition. As in our previous work for determining the vapour-liquid interfacial properties of binary mixtures of LJ molecules, we have also determined the components of the pressure tensor of the symmetrical LJ mixture using an alternative approach. We follow the methodology proposed by de Miguel and Jackson,[9] based on the seminal works of Eppenga and Frenkel[58] and Harismiadis *et al.*,[59] and use virtual volume perturbations of magnitude $\xi = \Delta V/V$ every five MC cycles. Here, ξ defines the relative volume (compressive and expansive) change associated with the perturbation, i.e., rescale independently the box lengths of the simulation cell and positions of the molecular centers of mass according to linear transformations along the appropriate directions. In all cases, eight different (positive and negative) relative volume changes in the range $2 \times 10^{-4} \leq |\xi| \leq 15 \times 10^{-4}$ are used in our calculations. The final values of the macroscopic components of the pressure tensors presented in this work, P_N and P_T, correspond to the extrapolated values (as determined by a linear extrapolation to $|\xi| \to 0$ of the values obtained from increasing-volume and decreasing-volume perturbations) obtained from a combined compression-expansion perturbation.

Similarly, surface tension is determined using three independent routes. In the first one, we use the mechanical definition that involves the integration of the difference between the tangential and normal microscopic components of the pressure tensor profiles, as obtained from the IK methodology. In the second route, the surface tension is calculated using the thermodynamic definitions of P_N and P_T, as proposed by de Miguel and Jackson.[9] Finally, in the third route, we use TA methodology.[3] Since the method is a standard and well-known procedure for evaluating fluid-fluid interfacial tensions of molecular systems, here we only provide the most important features of the technique. For further details, we recommend the original work[3] and the most important applications.[7,9,16,19–24,27,28,33,34,44,60–62] The implementation of the TA technique involves performing virtual or test area deformations of relative area changes defined as $\xi = \Delta\mathcal{A}/\mathcal{A}$ during the course of the simulation at constant N, V, and T every five MC cycles. Note that the procedure for calculating the surface tension is similar to that used to evaluate the components of the pressure tensor, but in this case the changes in the normal and transverse dimensions are coupled to keep the overall volume constant. In particular, we use the same number and values for the relative area changes ξ, and the same procedure to obtain the extrapolated values.

In this work, we consider six reduced pressures in the range $P^* = P\sigma^3/\epsilon \approx 1.5$ up to 3.5 for each cut-off distance used. In the case of $NP_z\mathcal{A}T$ simulations of the homogeneous liquid phases prepared in the first step, each simulation box is equilibrated for 10^6 MC cycles. In the case of the NVT simulations corresponding to the interfacial box, the system is also well equilibrated for other 10^6 equilibration MC cycles. In addition to that, averages are determined over a further period of 2×10^6 MC cycles. The production stage is divided into M blocks. Normally, each block is equal to 10^5 MC cycles. The ensemble average of the macroscopic components of the pressure tensor and the surface tension is given by the arithmetic mean of the block averages and the statistical precision of the sample average is estimated from the standard deviation in the ensemble average from $\overline{\sigma}/\sqrt{M}$, where $\overline{\sigma}$ is the variance of the block averages, and $M = 20$ in all cases.

From this point, all the quantities in our paper are expressed in conventional reduced units of component 1, with σ and ϵ being the length and energy scaling units, respectively. Thus, the temperature is given in units of ϵ/k_B, the densities of both components and the total density in units of σ^{-3}, the bulk pressure and components of the pressure tensor in units of the ϵ/σ^3, the surface tension in units of ϵ/σ^2, and the distances, including the cut-off radius, in units of σ.

III. RESULTS AND DISCUSSION

In this section, we present the main results from simulations of the liquid-liquid interface of a symmetrical mixture of spherical LJ molecules using different cut-off distances and LRC for the intermolecular potential energy and components of the pressure tensor. We focus mainly on the effect of the cut-off distance of the intermolecular potential on several interfacial properties. As in our previous works,[34,35] we have determined the components of the pressure using both the mechanical (or virial) and thermodynamic routes. Comparison between both results allows to check the validity of the method presented in the previous works[7,34,35,44] for determining the contribution to the energy and pressure due to the LRC in mixtures of LJ systems. We now extend the methodology to deal with liquid-liquid interfaces. We also examine the phase equilibria of the mixture, including pressure-density or $P\rho$, and pressure-composition or Px, projections of the phase diagram at a given temperature. In addition to that, we also analyze the most important interfacial properties, such as density profiles and interfacial tension. As in our previous works for pure and binary mixtures,[34,35] in which we concentrate on vapour-liquid interfaces, we now pay special attention on the determination of the liquid-liquid interfacial tension calculated using different routes, including the mechanical or virial route (using the traditional IK methodology) and the thermodynamic definition (using the VP and TA methods) of the surface tension.

It is important to recall here that, although the major difference between liquid and vapour phases from a macroscopic point of view is density, from a microscopic view both phases are radically different. Whereas in a vapour phase correlation between molecules, separated distances beyond 2σ approximately, being σ the molecular diameter of the molecular specie, liquids, especially at high densities, exhibit large correlations that strongly affect macroscopic properties. Many of those properties, with particular emphasis on interfacial properties such as interfacial tension, are extremely sensible to such molecular details. As we have mentioned explicitly in the Introduction, one of the main goals of the present work is to establish clearly if inhomogeneous LRC to the potential energy and pressure and perturbative methods based on a thermodynamic perspective are suitable for predicting interfacial properties of this kind of mixture.

We apply the methodology explained in Section II to the model previously presented. As we have mentioned, the system is a limiting case of a mixture in which both components are

identical, i.e., the molecules of both components have the same molecular sizes and dispersive energy interactions. However, the unlike dispersive energy between unlike components is half of the pure components. In order to clarify the nature of the phase behavior exhibited by the system under study, we present the phase diagram of the mixture as obtained from the well-known soft-SAFT approach.

The pressure-temperature PT projection of the PTx surface corresponding to the phase diagram of the symmetrical mixture of LJ spheres is shown in Fig. 1. It is interesting to mention here that Jackson,[63] in early 1990s, studied a binary mixture of equal-sized hard spheres with mean-field attractive forces between like species and not between unlike species using the SAFT equation of state. The phase diagram of that mixture is similar to that obtained here from the soft-SAFT approach. The continuous black curves are the vapour pressure curves of pure components 1 and 2, which are coincident for the mixture due to its symmetry. As can be seen, the system exhibits a liquid-liquid-vapour (LLV) three-phase line (green dashed curve), located at pressures above the vapour pressure curves of pure components. In addition to that, the mixture has two critical lines with different characters. The first one is a gas-liquid critical line (dotted-dashed red curve), running from the critical point of pure components 1 and 2 to a tricritical point (TCP). The second one is a liquid-liquid critical line (dotted-dotted-dashed blue curve), running from the TCP of the mixture toward high pressures and temperatures. The PT projection of the phase diagram is characterized by two salient features. First, the phase behavior of the mixture is dominated by a large liquid-liquid immiscibility region extending left of the liquid-liquid critical line and three-phase line. Second, there is the unusual occurrence of a TCP in a binary mixture, at $T \approx 1.442$ and $P \approx 0.596$. A TCP is a thermodynamic state at which three coexisting phases become identical. Note that the existence of this critical state is a consequence of the symmetrical nature of the interactions, since the rule phase forbids unsymmetrical TCPs in systems with less than three components. In fact, TCPs appear in either ternary mixtures at an unique temperature and pressure or in quaternary mixtures at fixed pressure and unique temperature. For details about TCPs, we recommend the work of Vega and Blas[64] and references therein. According to the classification of Scott and van Konynenburg,[65,66] the phase diagram corresponding to the mixture is just the symmetrical limit of type III phase behavior with heteroazeotropy or simple type III-HA.

To better understand the phase behavior exhibited by the mixture, it is also useful to examine the pressure-composition Px or temperature-composition Tx projections of the PTx surface of the phase diagram. Fig. 2 shows the Px constant-temperature projection at different temperatures. Part (a) of the figure shows the Px projection at $T = 1.25$, below the critical point of pure components. As can be seen, the system

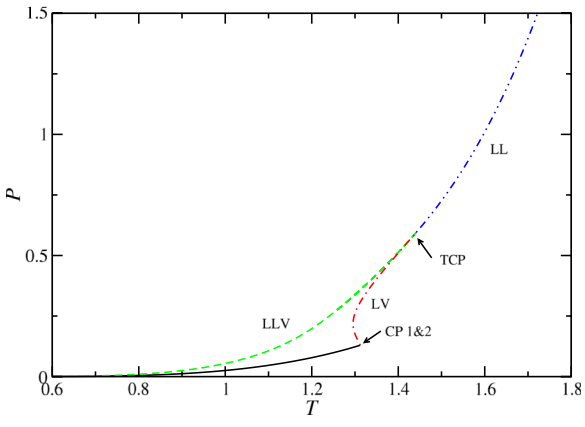

FIG. 1. PT projection of the phase diagram for the symmetrical mixture of LJ molecules with different dispersive energies between unlike species, $\epsilon_{12} = 0.5\epsilon$, as obtained from the soft-SAFT theoretical formalism. Continuous black curves represent the vapour pressure of the pure components (1 and 2), the dashed green curve represents the LLV three-phase line, the dotted-dashed red curve is the vapour-liquid (VL) critical line, and the dotted-dotted-dashed curve is the liquid-liquid (LL) critical line. TCP denotes the tricritical point of the mixture.

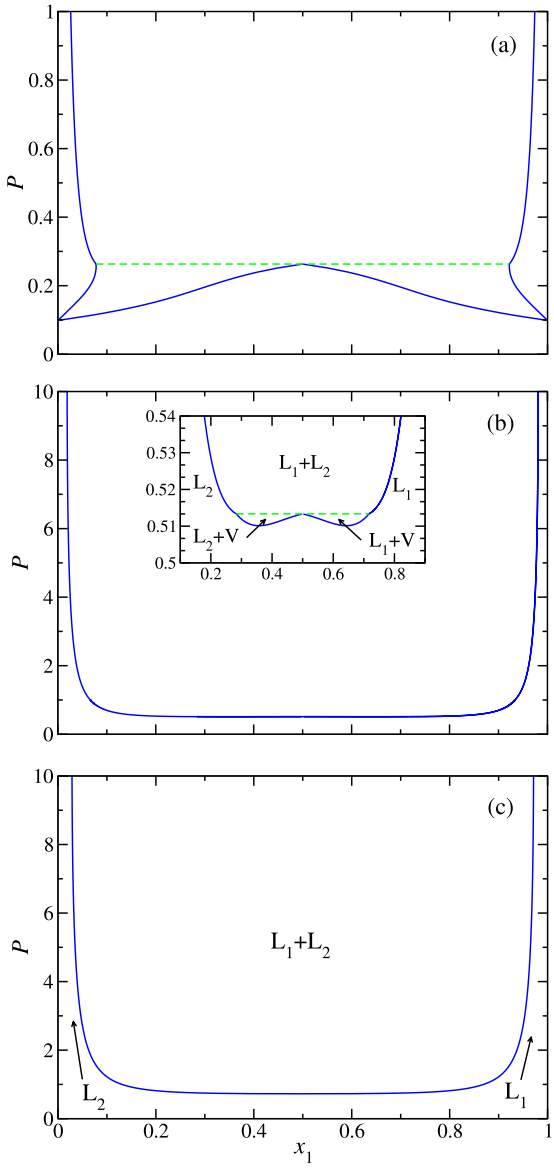

FIG. 2. Px projection of the phase diagram for the symmetrical mixture of LJ molecules with different dispersive energies between unlike species, $\epsilon_{12} = 0.5\epsilon$, as obtained from the soft-SAFT theoretical formalism at reduced temperatures (a) $T = 1.25$, (b) $T = 1.4$, and (c) $T = 1.5$. Continuous green curves represent the vapour-liquid (VL) and liquid-liquid (LL) phase envelopes and the dashed green curves correspond to the LLV three-phase line at the corresponding pressure.

exhibits two equivalent vapour-liquid coexistence regions (due to the symmetry of the mixture) at low pressures, below the three-phase coexistence at $P \approx 0.263$, and liquid-liquid immiscibility at high pressures. We have also studied the Px projection of the phase diagram at $T = 1.4$, a temperature above the critical temperature of pure components, but below the tricritical temperature of the mixture, $T_{TCP} \approx 1.442$, as shown in part (b) of the figure. The system also exhibits two equivalent vapour-liquid envelopes, since the temperature is above the critical point of pure components, and liquid-liquid phase separation at high pressures. Finally, at $T = 1.5$, above the tricritical point of the mixture, the vapour-liquid coexistence has merged into the liquid-liquid coexistence and only liquid-liquid immiscibility is stable at these conditions, as it is shown in part (c) of the figure.

Once we have obtained a general picture of the complete phase diagram of the mixture, we consider the most important interfacial properties of the system. We first analyze the effect of the cut-off distance of the intermolecular potential energy on density profiles. We follow a similar analysis and methodology than in our previous works[7,16,34,35,44,60] and consider different cut-off distances and pressures. The equilibrium density profiles of each of the components of the mixture, $\rho_1(z)$ and $\rho_2(z)$, as well as the total density, $\rho(z) = \rho_1(z) + \rho_2(z)$, are computed from averages of the histogram of densities along the z direction over the production stage. The bulk vapour and liquid densities of both components and the total density are obtained by averaging $\rho_1(z)$, $\rho_2(z)$, and $\rho(z)$, respectively, over appropriate regions sufficiently removed from the interfacial region. The densities obtained are meaningful since the central liquid slab is thick enough at all pressures. The bulk vapour densities are obtained after averaging the corresponding density profiles on both sides of the liquid film. The statistical uncertainty of these values is estimated from the standard deviation of the mean values.

Our simulation results for the bulk densities of each component, total densities, molar fractions of both components in each phase, components of the pressure tensor, and surface tension for symmetrical mixtures of LJ molecules interacting with the Lennard-Jones intermolecular potential using different cut-off distances, at different pressures, are collected in Tables I and II.

We show in Fig. 3 the density profiles $\rho_1(z)$, $\rho_2(z)$, and $\rho(z)$ for the mixture of LJ molecules using cut-off distances $r_c = 3$ and 4, and $r_c = 3$ with inhomogeneous LRC, at several pressures. For the sake of clarity, we only present one half of the profiles corresponding to one of the interfaces. Also for convenience, all density profiles have been shifted along z so as to place z_0, the position of the Gibbs-dividing surface, approximately at the origin. As can be seen, the density profiles of both components along the interface are perfectly symmetric. The bulk density of one of the components in one of the liquid phases is identical to the other in the second phase liquid, and hence, the compositions of both components are also symmetric (see the details in Table I). This is a consequence of the symmetrical nature of the interactions

TABLE I. Total liquid density at liquid phases L_1 and L_2, ρ, density of component 1 at liquid L_1, $\rho_1^{L_1}$, density of component 1 at liquid L_2, $\rho_1^{L_2}$, molar composition of component 1 at liquid L_1, $x_1^{L_1}$, molar composition of component 1 at liquid L_2, $x_1^{L_2}$, density of component 2 at liquid L_1, $\rho_2^{L_1}$, density of component 2 at liquid L_2, $\rho_2^{L_2}$, at $T = 1.5$ and different pressures P_N^{vir} for the symmetrical mixture of LJ molecules with different dispersive energies between unlike species, $\epsilon_{12} = 0.5\epsilon$, at $T = 1.5$ and using a cut-off distance for the intermolecular potential (a) $r_c = 3$, (b) $r_c = 4$, and (c) $r_c = 3$ with inhomogeneous long-range corrections. All quantities are expressed in the reduced units defined in Section II. The errors are estimated as explained in the text.

P_N^{vir}	ρ	$\rho_1^{L_1}$	$\rho_1^{L_2}$	$x_1^{L_1}$	$x_1^{L_2}$	$\rho_2^{L_1}$	$\rho_2^{L_2}$
			$r_c = 3.0$				
1.7349(14)	0.6730(5)	0.5644(18)	0.105 9(4)	0.838(5)	0.1573(7)	0.1086(15)	0.567 3(6)
1.9405(18)	0.6946(21)	0.6034(17)	0.098 9(9)	0.868(4)	0.1427(14)	0.0917(6)	0.594 6(11)
2.1724(20)	0.7149(20)	0.6330(18)	0.087 6(6)	0.885(4)	0.1226(8)	0.0820(8)	0.627 2(7)
2.6921(21)	0.7511(22)	0.6745(19)	0.071 7(3)	0.898(5)	0.0954(4)	0.0762(5)	0.680 0(4)
3.1403(16)	0.7774(12)	0.7114(12)	0.069 3(5)	0.915(3)	0.0893(7)	0.0663(8)	0.707 4(6)
3.6735(24)	0.802(3)	0.7312(20)	0.076 81(22)	0.911(5)	0.0958(5)	0.0710(4)	0.724 5(3)
			$r_c = 4.0$				
1.6251(13)	0.6736(19)	0.5889(17)	0.088 0(5)	0.874(4)	0.1307(8)	0.0847(6)	0.585 3(7)
1.9053(12)	0.7025(7)	0.6302(14)	0.074 3(4)	0.897(3)	0.1059(6)	0.0725(11)	0.627 6(8)
2.0229(19)	0.7112(21)	0.6330(18)	0.073 3(6)	0.890(5)	0.1031(9)	0.0782(4)	0.637 7(7)
2.6818(19)	0.7577(22)	0.6935(21)	0.065 6(4)	0.915(5)	0.0866(6)	0.0641(6)	0.692 1(5)
2.9951(18)	0.775(3)	0.7159(21)	0.061 3(5)	0.923(5)	0.0790(7)	0.0598(4)	0.713 8(7)
3.6535(19)	0.807(3)	0.7472(20)	0.056 1(6)	0.926(5)	0.0695(8)	0.0593(3)	0.751 0(7)
			$r_c = 3.0 + LRC$				
1.5510(13)	0.6713(7)	0.5912(6)	0.086 59(15)	0.8797(16)	0.1293(3)	0.0805(3)	0.583 21(23)
1.8634(14)	0.7039(21)	0.6346(19)	0.068 1(3)	0.902(5)	0.0968(5)	0.0692(5)	0.635 9(5)
2.1423(14)	0.7265(23)	0.6626(24)	0.063 3(5)	0.912(5)	0.0871(7)	0.0640(8)	0.662 9(7)
2.6045(16)	0.7569(22)	0.6955(20)	0.059 89(22)	0.919(5)	0.0791(3)	0.0611(4)	0.697 5(3)
3.0826(20)	0.7842(8)	0.7327(10)	0.055 6(3)	0.9342(20)	0.0709(4)	0.0516(7)	0.728 2(4)
3.3374(16)	0.7964(24)	0.7455(23)	0.051 3(3)	0.936(5)	0.0644(3)	0.0508(7)	0.745 2(3)

TABLE II. Normal component of the macroscopic pressure tensor calculated from the virial route P_N^{vir}, normal and tangential components of the macroscopic pressure tensor calculated from VP, P_N, and P_T, interfacial tension calculated from integration given by Eq. (1), γ^{vir}, from VP, γ_{VP}, and from TA, γ_{TA}, at $T = 1.5$ and different pressures for the symmetrical mixture of LJ spherical molecules with different dispersive energies between unlike species, $\epsilon_{12} = 0.5\epsilon$, at $T = 1.5$ and using a cut-off distance for the intermolecular potential (a) $r_c = 3$, (b) $r_c = 4$, and (c) $r_c = 3$ with inhomogeneous long-range corrections. All quantities are expressed in the reduced units defined in Section II. The errors are estimated as explained in the text. Uncertainties of interfacial tension calculated from the virial route, γ^{vir}, are error estimates corresponding to the numerical calculation of the integral given by Eq. (1).

P_N^{vir}	P_N^*	P_T^*	γ^{vir}	γ_{VP}	γ_{TA}
		$r_c = 3.0$			
1.7349(14)	1.7344(16)	1.7288(17)	0.116(6)	0.11(4)	0.118(3)
1.9405(18)	1.9408(11)	1.9329(11)	0.159(6)	0.16(3)	0.159(4)
2.1724(20)	2.1727(12)	2.1625(13)	0.197(5)	0.20(3)	0.199(5)
2.6921(21)	2.6924(7)	2.6783(8)	0.282(8)	0.285(22)	0.284(9)
3.1403(16)	3.1407(7)	3.1251(7)	0.310(8)	0.315(20)	0.313(6)
3.6735(24)	3.6736(13)	3.6539(13)	0.395(6)	0.39(3)	0.397(8)
		$r_c = 4.0$			
1.6251(13)	1.6253(13)	1.6157(14)	0.187(6)	0.19(4)	0.189(5)
1.9053(12)	1.9054(9)	1.8933(9)	0.244(6)	0.24(2)	0.245(4)
2.0229(19)	2.0228(11)	2.0094(12)	0.272(6)	0.27(3)	0.274(6)
2.6818(19)	2.6821(13)	2.6632(14)	0.374(6)	0.37(3)	0.376(5)
2.9951(18)	2.9951(9)	2.9747(10)	0.411(7)	0.41(3)	0.414(6)
3.6535(19)	3.6537(5)	3.6301(6)	0.466(8)	0.472(17)	0.469(9)
		$r_c = 3.0 + LRC$			
1.5510(13)	1.5431(12)	1.5317(12)	0.236(6)	0.23(3)	0.229(6)
1.8634(14)	1.8537(13)	1.8381(14)	0.311(6)	0.31(3)	0.313(5)
2.1423(14)	2.1317(11)	2.1122(11)	0.390(5)	0.39(3)	0.390(5)
2.6045(16)	2.5958(8)	2.5725(9)	0.468(7)	0.47(3)	0.461(8)
3.0826(20)	3.0761(7)	3.0495(8)	0.550(11)	0.535(22)	0.535(7)
3.3374(16)	3.3251(6)	3.2954(5)	0.580(7)	0.601(17)	0.596(8)

of the system. As can be seen, for a given value of the cut-off distance of the intermolecular potential, the slope of the density profiles corresponding to both components in the interfacial region increases as the pressure is increased, making larger the jump in densities when passing from one liquid phase to the other liquid phase of the interface. Consequently, the interfacial thickness increases, an expected behavior that indicates the phase envelope is becoming thinner as the pressure increases with respect to the critical pressure of the mixture. It is important to recall that the critical pressure of the mixture, at $T = 1.5$, is $P \sim 0.727$ as predicted by the soft-SAFT approach, well below the pressures considered here.

Special attention deserves the behavior of the total density profile. As we have mentioned before, the bulk liquid total densities associated to both liquid phases are identical, as can be also seen in Table I. However, the total density profile, $\rho(z) = \rho_1(z) + \rho_2(z)$, which is nearly constant in the bulk region of the liquid phases, exhibits a local minimum at the interface, when passing from one liquid phase to the other. This minimum is obviously related with a desorption of both components at the interface. We think this phenomenon is a combination of the weak dispersive interactions between unlike species of the mixture and the presence of an interfacial region, that separates the two immiscible liquid phases in

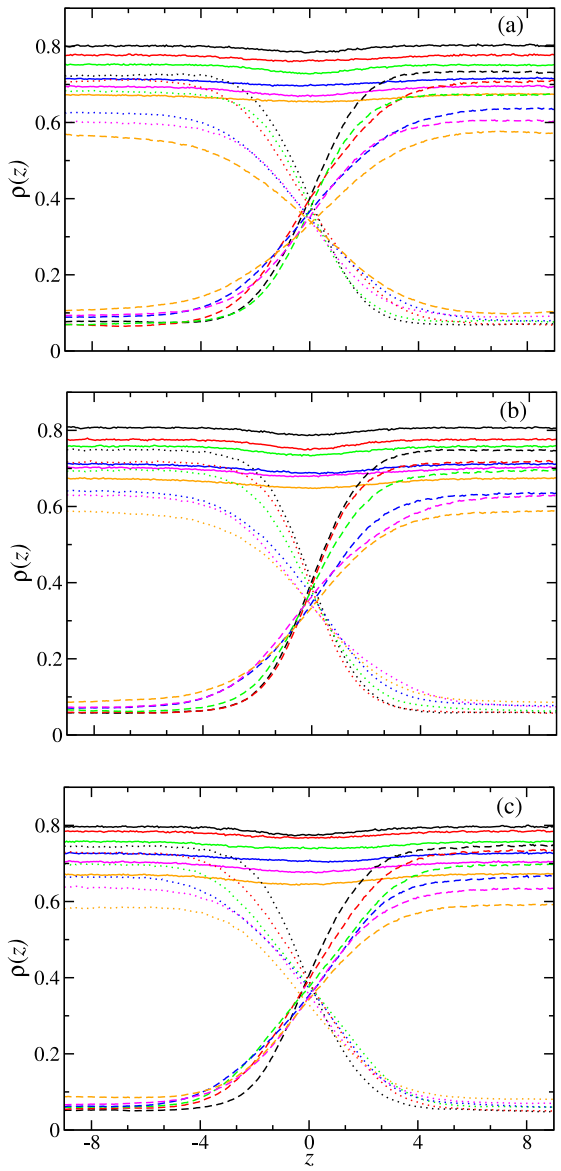

FIG. 3. Simulated equilibrium total density profiles (continuous curves), density profiles of component 1 (dotted curves), and density profiles of component 2 (dashed curves) across the liquid-liquid interface of the symmetrical mixture of LJ molecules with different dispersive energies between unlike species, $\epsilon_{12} = 0.5\epsilon$, at $T = 1.5$ and using a cut-off distance for the intermolecular potential (a) $r_c = 3$, (b) $r_c = 4$, and (c) $r_c = 3$ with inhomogeneous LRC. Pressure of the system increases from bottom to top in the total density profile (orange, magenta, blue, green, red, and black). Note that curves with the same colour correspond to the same pressure value.

coexistence, in which molecules of both components must accommodate in order to minimize the free energy of the system. A similar behavior has been previously observed for liquid-liquid interfaces in partially miscible mixtures of LJ-like systems from MD simulation[67–69] and density functional theory.[69,70]

From a phase equilibria perspective, preferential adsorption or desorption of one of the components of a heterogeneous mixture can also be understood in terms of molar barotropy phenomena and the existence of isopycnic states. Molar density inversion, a phenomenon also known as molar barotropy, corresponds to a singular behavior that occurs when molar densities of two immiscible liquid phases in equilibrium

change their relative position of phases in the heterogeneous mixture. The points of the diagram at which both liquid phases exhibit equal molar densities of volume are called isopycnic states.[71–73] Experimentally, these phenomena may be observed when varying the equilibrium conditions of temperature or pressure. From an experimental point of view, molar density inversions are likely to occur in partially miscible mixtures that exhibit type III or type V phase behavior according to the Scott and van Konynenburg classification.[65,66] In particular, isopycnic curves, along which the phase density inversions take place, are clearly observed to occur in an equilibrium range that goes from the LLV three-phase line up to the vapour-liquid critical line of the mixture.[74] In this work, due to the symmetrical nature of the interactions, molar density of both phase liquids at the LLV coexistence line is identical, and hence, all the states along the three-phase line are isopycnic states.

Tardón *et al.*[74] have demonstrated recently from computer simulation and the use of the density gradient theory that this particular phase behavior of mixtures that exhibit liquid-liquid immiscibility produces a drastic distortion of the total density profile of the system along the liquid-liquid interface. We think the desorption phenomena observed in the total density profile of the mixture shown in Fig. 3 should be related to the existence of isopycnic states at which two liquids coexist with the same molar density. Since the goal of this work is not to investigate this delicate and interesting phenomena, we plan to carry out a detailed study of the effect of isopycnity of symmetrical binary mixtures of equal-sized LJ spheres from a computer simulation approach in a future work.

Comparison of Figs. 3(a)–3(c) also shows the effect of increasing the cut-off distance of the intermolecular potential energy, $r_c = 3$ and 4, and the use of inhomogeneous LRC with $r_c = 3$ (full intermolecular potential). As can be seen, an increase of cut-off distance results in steeper density profiles of both components along the interfacial region. This effect, which also produces narrower interfacial regions, is related with the increasing of the interfacial tension of the mixture, as it will be shown later. As more interactions are taken into account, the unlike intermolecular interactions are larger, and the *Px* pressure-composition phase envelope (see Fig. 2) becomes wider in terms of molar fractions, or in other words, the jump in composition increases when going from one liquid phase to the other one.

Note that this behavior is not easy to identify from Fig. 3 since, although simulated pressures are approximately equal, they are, in fact, not identical since we have simulated the interface using the *NVT* or canonical ensemble. Under these conditions, pressure is not specified *a priori* but it is calculated along the simulation. Although initial simulation boxes are prepared carefully trying to ensure the same final values of the pressure, small differences are nearly impossible to avoid (see Tables I and II for further details). Obviously, since we are dealing with a binary mixture, the use of the $NP_z\mathcal{A}T$ or isothermal-isobaric ensemble in which the normal pressure (perpendicular to the liquid-liquid interface) is kept constant seems to be a more appropriate ensemble than the standard *NVT* ensemble. We have not used the $NP_z\mathcal{A}T$ ensemble because the precise composition between different density profiles at exactly the same pressure was not the primary goal of this work. However, we plan to use this ensemble in future works.

The liquid-liquid phase envelopes of the mixture of LJ molecules using different cut-off distances for the intermolecular potential, r_c, including the full potential as calculated from the analysis of the density profiles obtained from our Monte Carlo simulations, are depicted in Fig. 4. The soft-SAFT theoretical approach has been also used to obtain the complete phase diagram of the symmetrical mixture for the full potential case. Although, as we have mentioned in the Introduction and Sec. II that we have used the information from the theory for obtaining initial guesses of the liquid and vapour densities and compositions of mixtures to be studied by simulation at particular thermodynamic conditions, these theoretical predictions can also be used as results to compare our simulation results and check the ability of SAFT in predicting the phase behavior of these mixtures. As can be seen in part (a) of the figure, the pressure-density or $P\rho$ projection of the phase diagram of mixture, at $T = 1.5$, only exhibits one branch of the liquid-liquid coexistence diagram. As it has been explained previously in the case of the *PT* projection of the phase diagram, this is a direct consequence of the symmetrical nature of the interactions of the system. In

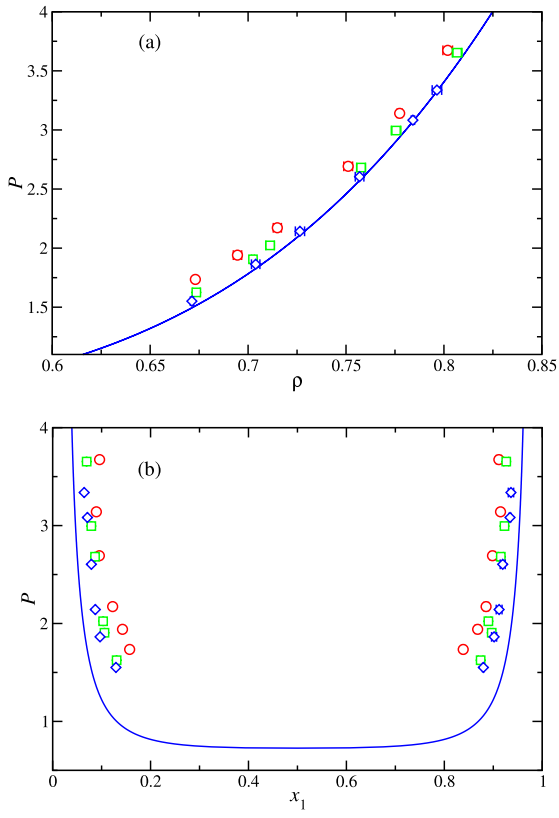

FIG. 4. Pressure-density or $P\rho$ (a) and pressure-composition or *Px* (b) projections projection of the phase diagram of the symmetrical mixture of LJ molecules with different dispersive energies between unlike species, $\epsilon_{12} = 0.5\epsilon$, at $T = 1.5$ and using a cut-off distance for the intermolecular potential $r_c = 3$ (red circles), $r_c = 4$ (green triangles), and $r_c = 3$ with inhomogeneous long-range corrections (blue squares). Symbols correspond to simulation data obtained in this work and curves are the predictions obtained from the soft-SAFT theoretical formalism.

other words, both curves collapse in a unique coexistence curve since the densities of each of the liquid phases are identical.

The coexistence densities of both phases increase as the pressure of the system is increased, an expected behavior due to the compression effect. In addition to that, at each pressure considered, the coexistence densities increase as the intermolecular potential cut-off distance r_c is increased. This enlargement of the liquid coexistence density associated to the phase envelope is essentially due to the increase of the attractions in the system (r_c is increased) as more interactions are taken into account. This increasing behavior has an asymptotic limiting behavior associated to the case in which all attractive interactions are taken into account, i.e., when considering the full intermolecular potential. As can be seen, agreement between Monte Carlo simulation results obtained using the inhomogeneous LRC (full potential) and predictions from SAFT is excellent in all cases. It is important to recall here that results from the theory are predictions without any further fitting procedure.

We have also obtained the pressure-composition or Px projection of the mixture at the same thermodynamic conditions and using the same cut-off distances for the intermolecular potential energy, including the case in which the inhomogeneous LRC are used. As can be seen in part (b) of the figure, we have presented the molar fractions of the mixture from the analysis of the density profiles, as well as the predictions obtained from the soft-SAFT. The phase diagrams for cases in which different cut-off distances are used show the expected behavior, in agreement with part (a) of the figure. In particular, the phase separation of the mixture increases as the pressure is increased. In addition to that, the coexistence compositions in both liquid phases, at a given pressure, increase as the cut-off distance of the intermolecular potential energy is increased (higher values of r_c). As can be seen, the liquid-liquid immiscibility region of the phase diagram of the symmetrical mixture increases in compositions as pressure is increased, an expected behavior of mixtures that exhibit type III phase behavior according to the classification of Scott and van Konynenburg.[65,66] Agreement between Monte Carlo simulation and theoretical predictions is good when the full intermolecular potential is taken into account through the inhomogeneous LRC. Again, it is important to recall here that no single adjustable parameter has been used to obtain the prediction from the soft-SAFT theoretical formalism.

Once we have studied the phase equilibria properties of the mixture from the analysis of the density profiles, we now turn on the study of the liquid-liquid interfacial tension of the mixture using different values of the cut-off distance for the intermolecular potential energy and the inhomogeneous LRC of MacDowell and Blas[7] and Blas and Martínez-Ruiz.[34,35] In particular, we have determined the liquid-liquid interfacial tension using its mechanical definition that involves the integration of the difference between the tangential and normal microscopic components of the pressure tensor profiles, as obtained from the IK methodology, along the simulation box (Eq. (1)). In addition to that, we have also determined the interfacial tension using two perturbative approaches: the TA method of Gloor *et al.*[3] and the VP technique of de Miguel and Jackson.[9] In the first case, the surface tension is determined performing virtual area perturbations of a small magnitude during the course of the simulation at constant volume. In the second case, the surface tension is determined in two steps. In the first step, the normal and tangential macroscopic components of the pressure tensor, P_N and P_T, are calculated from their thermodynamic definitions as proposed by de Miguel and Jackson.[9] In the second step, the surface tension γ is obtained from Eq. (21) of the work of de Miguel and Jackson.[9]

The calculation of the surface tension through three different but complementary routes allows to compare the results obtained from the mechanical and thermodynamic methods. This is another convincing test for consistency for the inhomogeneous LRC presented in our previous works for mixtures. Note that similar consistent results have been found in the previous applications of the method for calculating the total potential energy of the system.[7,34,44,60] This is the first time the inhomogeneous LRC for both the intermolecular energy and pressure tensor are used to predict the liquid-liquid interfacial properties of mixtures, and to our knowledge, this is also the first time the volume perturbation methodology proposed by de Miguel and Jackson[9] for determining the components of the pressure tensor is used to deal with liquid-liquid interfaces.

The pressure dependence of the interfacial tension for the mixture interacting with different cut-off distances for the intermolecular potential is shown in Fig. 5. Agreement between our independent simulations demonstrates that both methodologies are fully equivalent for all the systems and conditions studied. As can be seen, at any given pressure, the interfacial tension is larger for simulations in which the cut-off distance is larger, and, in particular, for the simulations at which the inhomogeneous LRC are used. This latter case corresponds, as previously mentioned, to the case in which the full intermolecular potential is used. This behavior of the liquid-liquid interfacial tension is consistent with the larger cohesive energy in systems in which longer range of interactions is considered.

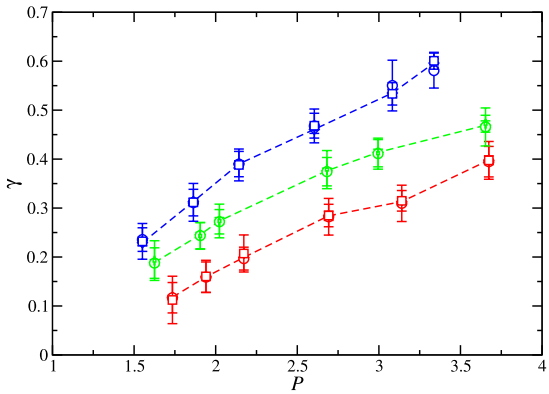

FIG. 5. Liquid-liquid interfacial tension as a function of pressure of the symmetrical mixture of LJ molecules with different dispersive energies between unlike species, $\epsilon_{12} = 0.5\epsilon$, at $T = 1.5$ and using a cut-off distance for the intermolecular potential $r_c = 3$ (red symbols), $r_c = 4$ (green symbols), and $r_c = 3$ with inhomogeneous long-range corrections (blue symbols). Different symbols represent the interfacial tension obtained from MC NVT simulations using the mechanical route of Irving and Kirkwood[8] (open circles), the VP method of de Miguel and Jackson[9] (open squares), and the TA technique[3] (open diamonds). The curves are included as guide to eyes.

IV. CONCLUSIONS

We have simulated the interfacial properties of the liquid-liquid interface of a symmetrical mixture of equal-sized spherical LJ molecules, with the same dispersive energy between like species, but with different dispersive energies between unlike species low enough to induce phase separation. The intermolecular interactions are truncated at two different cut-off distances for the intermolecular potential, $r_c = 3$ and 4σ, σ being the diameter of the molecules. In addition to that, inhomogeneous long-range corrections for dispersive interactions and pressure tensor are also used. The microscopic and macroscopic components of normal and tangential pressure are determined using two different routes, their mechanical (virial route) and thermodynamic (virtual pressure route) definitions. The interfacial tension is also evaluated using three different procedures, the Irving-Kirkwood method, the difference between the macroscopic components of the pressure tensor, and the test-area methodology. We have examined the density profiles and surface tension in terms of the pressure and the cut-off distance for the intermolecular potential energy, r_c. In addition, we have also calculated the coexistence diagram (pressure *versus* density) and the pressure-composition projection of the phase diagram at a constant temperature from an analysis of the density profiles.

The effect of the cut-off distance for the intermolecular potential energy of the symmetrical mixture on density profiles, microscopic components of the normal and tangential pressure tensor profiles, coexistence densities, and interfacial tension has been investigated. The liquid-liquid interface is seen to sharpen with increasing cut-off distance corresponding to an increase in the width of the coexistence phase envelope and the pressure-composition projection of the phase diagram and an accompanying increase in the surface tension.

ACKNOWLEDGMENTS

The authors would like to acknowledge helpful discussions with J. M. Garrido, J. M. Míguez, M. M. Piñeiro, and E. de Miguel. This work was supported by Ministerio de Economía y Competitividad through Grant No. FIS2013-46920-C2-1-P (confinanced with EU Feder funds). Further financial support from Junta de Andalucía and Universidad de Huelva is also acknowledged.

[1]J. S. Rowlinson and B. Widom, *Molecular Theory of Capillarity* (Claredon Press, 1982).
[2]F. Varnik, J. Baschnagel, and K. Binder, J. Chem. Phys. **113**, 4444 (2000).
[3]G. J. Gloor, G. Jackson, F. J. Blas, and E. de Miguel, J. Chem. Phys. **123**, 134703 (2005).
[4]L. G. MacDowell, J. Benet, and N. A. Katcho, Phys. Rev. Lett. **111**, 047802 (2013).
[5]L. G. MacDowell, J. Benet, N. A. Katcho, and J. M. Palanco, Adv. Colloid Interface Sci. **206**, 150 (2014).
[6]J. Janeček, J. Phys. Chem. B **110**, 6264 (2006).
[7]L. G. MacDowell and F. J. Blas, J. Chem. Phys. **131**, 074705 (2009).
[8]J. H. Irving and J. G. Kirkwood, J. Chem. Phys. **18**, 817 (1950).
[9]E. de Miguel and G. Jackson, J. Chem. Phys. **125**, 164109 (2006).
[10]E. de Miguel and G. Jackson, Mol. Phys. **104**, 3717 (2006).
[11]P. E. Brumby, A. J. Haslam, E. de Miguel, and G. Jackson, Mol. Phys. **109**, 169 (2010).
[12]L. G. MacDowell and P. Bryk, Phys. Rev. E **75**, 061609 (2007).
[13]A. P. Lyuvartsev, A. A. Martsinovski, S. V. Shevkunov, and P. N. Vorontsov-Velyaminov, J. Chem. Phys. **96**, 1776 (1992).
[14]J. R. Errington and D. A. Kofke, J. Chem. Phys. **127**, 174709 (2007).
[15]E. de Miguel, J. Phys. Chem. B **112**, 4647 (2008).
[16]F. J. Blas, L. G. MacDowell, E. de Miguel, and G. Jackson, J. Chem. Phys. **129**, 144703 (2008).
[17]G. Galliero, J. Chem. Phys. **133**, 074705 (2010).
[18]A. Ghoufi and P. Malfreyt, Mol. Simul. **39**, 603 (2013).
[19]C. Vega and E. de Miguel, J. Chem. Phys. **126**, 154707 (2007).
[20]J. M. Míguez, D. González-Salgado, J. L. Legido, and M. M. Piñeiro, J. Chem. Phys. **132**, 184102 (2010).
[21]G. Galliero, M. M. Piñeiro, B. Mendiboure, C. Miqueu, T. Lafitte, and D. Bessières, J. Chem. Phys. **130**, 104704 (2009).
[22]E. de Miguel, N. G. Almarza, and G. Jackson, J. Chem. Phys. **127**, 034707 (2007).
[23]C. Miqueu, J. M. Míguez, M. M. Piñeiro, T. Lafitte, and B. Mendiboure, J. Phys. Chem. B **115**, 9618 (2011).
[24]F. Biscay, A. Ghoufi, V. Lachet, and P. Malfreyt, J. Chem. Phys. **131**, 124707 (2009).
[25]A. Ghoufi, F. Goujon, V. Lachet, and P. Malfreyt, J. Chem. Phys. **128**, 154716 (2008).
[26]A. Ghoufi, F. Goujon, V. Lachet, and P. Malfreyt, Phys. Rev. E **77**, 031601 (2008).
[27]F. Biscay, A. Ghoufi, F. Goujon, and P. Malfreyt, J. Phys. Chem. B **112**, 13885 (2008).
[28]F. Biscay, A. Ghoufi, F. Goujon, V. Lachet, and P. Malfreyt, J. Chem. Phys. **130**, 184710 (2009).
[29]F. Biscay, A. Ghoufi, V. Lachet, and P. Malfreyt, Phys. Chem. Chem. Phys. **11**, 6132 (2009).
[30]J. C. Neyt, A. Wender, V. Lachet, A. Ghoufi, and P. Malfreyt, J. Chem. Phys. **139**, 024701 (2013).
[31]J. C. Neyt, A. Wender, V. Lachet, A. Ghoufi, and P. Malfreyt, J. Chem. Theory Comput. **10**, 1887 (2014).
[32]J. Benet, L. G. MacDowell, and C. Menduiña, J. Chem. Eng. Data **55**, 5465 (2010).
[33]R. de Gregorio, J. Benet, N. A. Katcho, F. J. Blas, and L. G. MacDowell, J. Chem. Phys. **136**, 104703 (2012).
[34]F. J. Martínez-Ruiz, F. J. Blas, B. Mendiboure, and A. I. Moreno-Ventas Bravo, J. Chem. Phys. **141**, 184701 (2014).
[35]F. J. Martínez-Ruiz and F. J. Blas, Mol. Phys. **113**, 1217 (2015).
[36]M. P. Allen, *Computer Simulation of Liquids* (Claredon, Oxford, 1987).
[37]D. Frenkel and B. Smit, *Understanding Molecular Simulations*, 2nd ed. (Academic, San Diego, 2002).
[38]E. M. Blokhius, D. Bedeaux, C. D. Holcomb, and J. A. Zollweg, Mol. Phys. **15**, 665 (1995).
[39]M. Mecke, J. Winkelmann, and J. Fischer, J. Chem. Phys. **107**, 9264 (1997).
[40]M. Mecke, J. Winkelmann, and J. Fischer, J. Chem. Phys. **110**, 1188 (1999).
[41]K. C. Daoulas, V. A. Harmandaris, and V. G. Mavrantzas, Macromolecules **38**, 5780 (2005).
[42]M. Guo and B. C.-Y. Lu, J. Chem. Phys. **106**, 3688 (1997).
[43]J. Janeček, H. Krienke, and G. Schmeer, J. Phys. Chem. B **110**, 6916 (2006).
[44]F. J. Blas, A. I. Moreno-Ventas Bravo, J. M. Míguez, M. M. Piñeiro, and L. G. MacDowell, J. Chem. Phys. **137**, 084706 (2012).
[45]M. S. Wertheim, J. Stat. Phys. **35**, 19 (1984).
[46]M. S. Wertheim, J. Stat. Phys. **35**, 35 (1984).
[47]M. S. Wertheim, J. Stat. Phys. **42**, 459 (1986).
[48]M. S. Wertheim, J. Stat. Phys. **42**, 477 (1986).
[49]E. A. Müller and K. E. Gubbins, Ind. Eng. Chem. Res. **40**, 2193 (2001).
[50]I. G. Economou, Ind. Eng. Chem. Res. **41**, 953 (2002).
[51]P. Paricaud, A. Galindo, and G. Jackson, Fluid Phase Equilib. **194**, 87 (2002).
[52]S. P. Tan, H. Adridharma, and M. Radosz, Ind. Eng. Chem. Res. **47**, 8063 (2008).
[53]C. McCabe and A. Galindo, in *Applied Thermodynamics of Fluids*, edited by A. R. H. Goodwin, J. V. Sengers, and C. J. Peters (Royal Society of Chemistry, Cambridge, 2010), Chap. 8, p. 215.
[54]J. K. Johnson, J. A. Zollweg, and K. E. Gubbins, Mol. Phys. **78**, 591 (1993).
[55]F. J. Blas and L. F. Vega, Mol. Phys. **92**, 135 (1997).
[56]F. J. Blas and L. F. Vega, Ind. Eng. Chem. Res. **37**, 660 (1998).
[57]A. Harasima, Adv. Chem. Phys. **1**, 203 (1957).
[58]R. Eppenga and D. Frenkel, Mol. Phys. **52**, 1303 (1984).
[59]V. I. Harismiadis, J. Vorholz, and A. Z. Panagiotopoulos, J. Chem. Phys. **105**, 8469 (1996).
[60]F. J. Blas, F. J. Martínez-Ruiz, A. I. Moreno-Ventas Bravo, and L. G. MacDowell, J. Chem. Phys. **137**, 024702 (2012).
[61]F. J. Blas and B. Mendiboure, J. Chem. Phys. **138**, 134701 (2013).
[62]J. M. Míguez, M. M. Piñeiro, and F. J. Blas, J. Chem. Phys. **138**, 034707 (2013).
[63]G. Jackson, Mol. Phys. **72**, 1365 (1991).

[64]L. F. Vega and F. J. Blas, Fluid Phase Equilib. **171**, 91 (2000).
[65]R. L. Scott and P. H. van Konynenburg, Discuss. Faraday Soc. **49**, 87 (1970).
[66]P. H. van Konynenburg and R. L. Scott, Philos. Trans. R. Soc. London, Ser. A **298**, 495 (1980).
[67]S. Toxvaerd and J. Stecki, J. Chem. Phys. **102**, 7163 (1995).
[68]E. Díaz-Herrera, J. Alejandre, G. Ramírez-Santiago, and F. Forstmann, J. Chem. Phys. **110**, 8084 (1999).
[69]P. Geysermans, N. Elyeznasni, and V. Russier, J. Chem. Phys. **123**, 204711 (2005).
[70]I. Napari, A. Laaksonen, V. Talanquer, and D. W. Oxtoby, J. Chem. Phys. **110**, 5906 (1999).
[71]S. Quiñones-Cisneros, Fluid Phase Equilib. **135**, 103 (1997).
[72]S. Quiñones-Cisneros, "Fluid phase equilibria from minimization of the free energy," M.Sc. Thesis, University of Minnesota (1987).
[73]M. E. Flores, M. J. Tardón, C. Bidart, A. Mejía, and H. Segura, Fluid Phase Equilib. **313**, 171 (2012).
[74]M. J. Tardón, J. M. Garrido, H. Quinteros-Lama, A. Mejía, and H. Segura, Fluid Phase Equilib. **336**, 84 (2012).